Pergamon

Tetrahedron 56 (2000) 6927–6943

TETRAHEDRON

Singlet Oxygen Mediated Oxidation of Olefins within Zeolites: Selectivity and Complexities

J. Shailaja,[a] J. Sivaguru,[a] Rebecca J. Robbins,[a] V. Ramamurthy,[a,*] R. B. Sunoj[b] and J. Chandrasekhar[b,*]

[a]*Department of Chemistry, Tulane University, New Orleans, LA 70118, USA*
[b]*Department of Organic Chemistry, Indian Institute of Science, Bangalore, 560012 India*

Received 11 February 2000; revised 26 March 2000; accepted 24 April 2000

Abstract—Thiazine dyes such as thionin, methylene blue and methylene green have been cation exchanged within monovalent cation exchanged Y zeolites. Depending on the water content, the dye molecules exist as either monomers ('dry') or dimers ('wet'). The monomeric dye, upon excitation with visible light, generates singlet oxygen, which has been utilized to oxidize alkenes to hydroperoxides. In the case of trisubstituted alkenes, hydroperoxidation within zeolites occurs with a certain amount of regioselectivity. The oxidation within zeolites is accompanied by photodecomposition of the dye and the product hydroperoxides and acid catalyzed rearrangement of the alkenes. In order to understand the observed selectivity, ab initio and DFT calculations on model systems have been performed. The calculations confirm fairly strong cation-alkene binding as well as additional geometric and orbital distortions. Computed activation energies for hydrogen abstraction suggest a significant rate retardation due to metal coordination. At both the MP2 and B3LYP levels, formation of the tertiary hydroperoxide by hydrogen abstraction from the methyl group (4-position) of 2-methyl 2-butene is calculated to be favored by a small margin. Between the gem-dimethyl units, abstraction from the *syn* methyl group is favored slightly compared to the *anti* counterpart. These predictions are not compatible with the observed regioselectivities. Further experimental and theoretical studies are underway to understand the observed regioselective oxidation within zeolites.

Introduction

One of the well known reactions of singlet oxygen is the hydroperoxidation of alkenes containing allylic hydrogens, often referred to as the 'ene' reaction.[1] Reaction with substrates containing several allylic hydrogens produces several distinct products (Scheme 1).[2] Although the peroxidation via singlet oxygen has found much synthetic application, regio- and stereo-control are still difficult issues.[3] The mechanistic details of the ene reaction are still being debated as well, however certain trends have been identified. Experiments by several groups have brought out the importance of the geometrical arrangement of the allylic hydrogens with respect to the attacking singlet oxygen during the hydroperoxide formation.[4] It has been established that for the ene reaction to occur the allylic C–H bond should be in plane with the π-orbital of the olefin. This led us to consider that, if one could control the conformation of the allylic substituent of the alkene and thus the accessibility of the allylic hydrogen(s) to the reagent, singlet

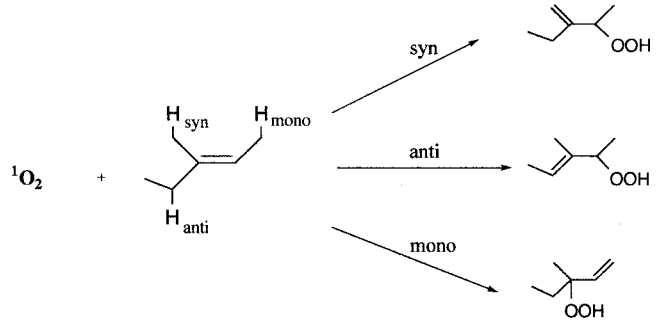

Scheme 1. Singlet oxygen during the ene reaction abstracts one of the three allylic hydrogens (*syn*, mono and *anti* H).

Keywords: thiazine dyes; Y zeolites; ene reaction.
* Corresponding authors. E-mail: murthy@mailhost.tcs.tulane.edu

0040–4020/00/$ - see front matter
PII: S0040-4020(00)00513-5

oxygen, one might be able to achieve selectivity in the oxidation reaction. It has been shown earlier that one can use zeolites as media to achieve conformational control in the case of aryl alkyl ketones and stilbenes.[5] In addition we reasoned that the presence of cations within a zeolite should alter the reactivity of zeolite-bound olefins by influencing the electron density distribution of the olefinic π-cloud. Further, we felt that the mechanistic details of singlet oxygen oxidation of cation bound olefins could be inherently interesting and significantly different from that of free olefins. In addition, current interest in environmentally benign oxidation processes could not be ignored.[6] With this background, we set out to explore the oxidation of a number of alkenes within Y zeolites.[7] When this study was initiated, to our knowledge, there was only one report of singlet oxygen initiated oxidation of alkenes within a zeolite.[8] Detailed studies carried out within zeolites in our[9] as well as other laboratories[10] have shown that hydroperoxidation of alkenes within zeolites can be regioselective. The results of our experimental as well as theoretical studies are presented below.

Results and Discussion

Dye sensitized oxidation of alkenes within a zeolite is complicated by several factors such as dye aggregation, poor photostability of dyes and photoproducts and the acid catalyzed rearrangements of the reactants and products. We therefore feel the experimental procedure and the various controls employed are critical to ascertaining the dependability of the observed selectivities during the oxidation of alkenes. In the context of regioselective oxidation, we have carried out a detailed study on two alkenes, 2-methyl-2-heptene and 1-methylcyclooctene within thionin, methylene blue and methylene green exchanged M^+Y zeolites (M^+=Li, Na, K, Rb and Cs). The results of this study are discussed in this report under the following subsections: (a) inclusion and characterization of dyes within M^+Y zeolites; (b) generation of singlet oxygen; (c) regioselective hydroperoxidation of 2-methyl-2-heptene and 1-methylcyclooctene; (d) complications due to poor stability of product hydroperoxides to light and oxygen; (e) complications due to poor stability of dyes to light and oxygen; (f) complications due to Brønsted acid sites and (g) theoretical studies on metal–olefin complexes.

Inclusion and characterization of dyes within M^+Y zeolites

Thiazine dyes thionin, methylene blue, and methylene green, when included within M^+ (M^+=Li, Na, K, Rb and Cs) Y zeolites were found to be useful as singlet oxygen sensitizers. Although dyes such as oxazine-1, oxazine-170, acridine orange, pyronin-Y, nile blue A, cresyl violet, methyl green, safranine, ethyl violet and basic Fuchsin could be introduced within a Y zeolite they were not useful as singlet oxygen sensitizers.[11] Therefore their inclusion within Y zeolites will not be discussed in this presentation. Cationic thiazine dyes were introduced into a M^+Y zeolite by the cation exchange process. A pictorial representation of the experimental protocol is provided in Scheme 2. The exchange involves placing the zeolite (~5 g *unactivated* M^+Y) in a prestirred aqueous solution of thionin (~5 mg in 250 mL of deionized water), continuous stirring for 24 h followed by filtration and aqueous washes (till the wash was

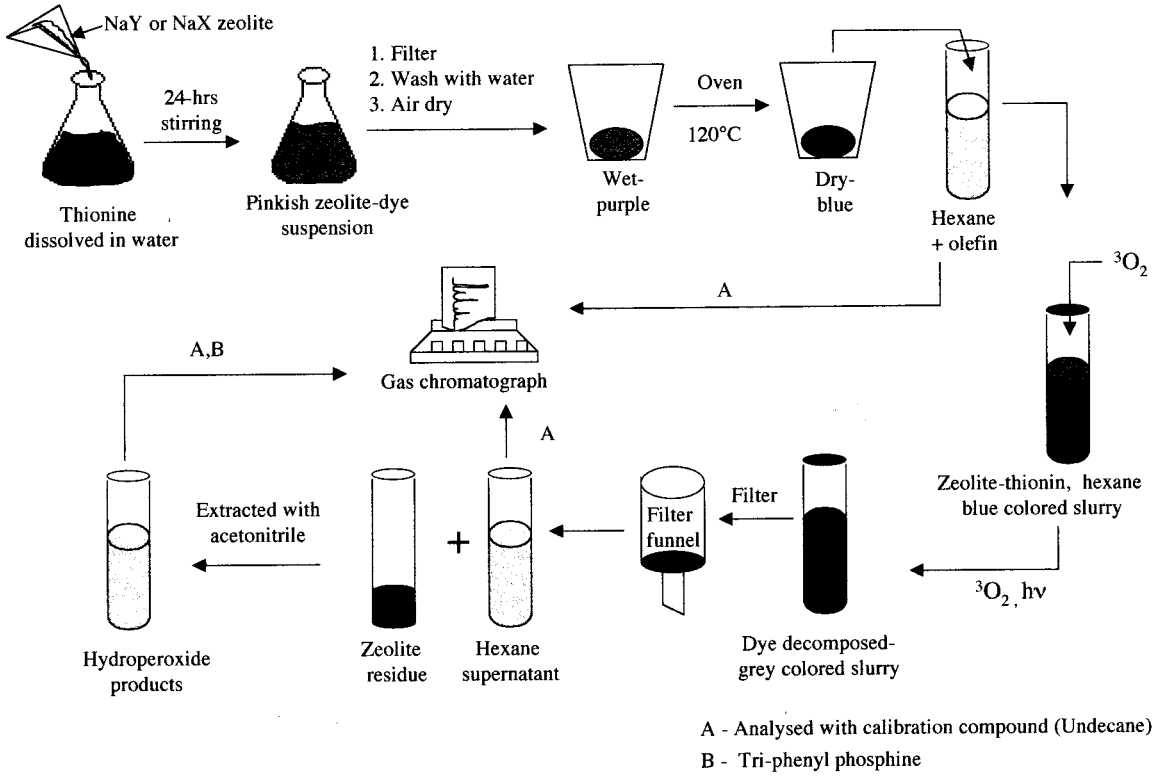

Scheme 2.

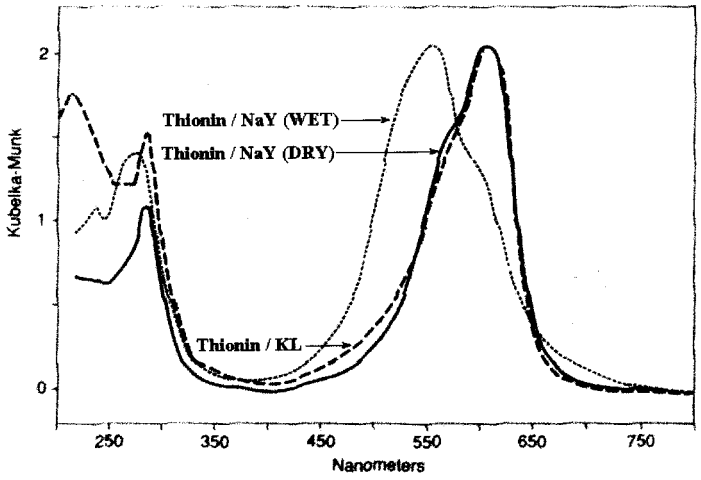

Figure. 1. Thionin in wet and dry NaY and in KL zeolites.

colorless) or Soxhlet extraction to yield a pink zeolite. Typically one dye molecule was present in every 150 supercages. However, obvious loss of dye during washes resulting in reduced amounts of dye included in 5 g of NaY must be noted. The pink thionin included zeolite was characterized by its diffuse reflectance spectrum (Fig. 1).

The presence of water in the zeolite has a dramatic effect on the state of aggregation of organic dyes within the zeolite cage. The diffuse reflectance spectrum of thionin exchanged NaY zeolite (pink in color) open to the atmosphere gave a λ_{max} at 545 nm. Upon drying under vacuum (10^{-3} Torr) with mild heating (~60°C), the zeolite turned blue and a shift to λ_{max} at 605 nm was observed (Fig. 1). We refer to the above treated sample as 'dry' even though it may still contain unknown amounts of water. Further drying at higher temperatures resulted in the decomposition of the dye. The two distinctly different adsorption maxima are characteristic of the monomer (605 nm) and H aggregates (545 nm).[12] Similar changes in color and absorption maxima were seen in the case of methylene blue (615–660 nm) and methylene green (570–650 nm) included in NaY. The diffuse reflectance spectral maxima of the monomers of thionin and methylene blue within Y zeolites were nearly independent of the cation (for thionin, methylene blue and methylene green the maximum in LiY, KY, RbY and CsY varied between 606 and 600, 675 and 660, and 645 and 655 nm, respectively). The diffuse reflectance spectrum of thionin included within KL zeolite is also shown in Fig. 1. In KL zeolite, owing to space constraints, thionin molecules exist as monomers only. Based on comparison of the spectra of the dye included NaY('dry') and KL samples[13] and the absorption spectrum of the dye in dilute aqueous solution[12] we conclude that under 'dry' conditions the dye molecules exist only as monomers within NaY.

Inclusion of thionin within M^{2+}(M=Mg, Ca, and Sr) Y zeolites resulted in an additional complication. Thionin was cation exchanged within M^{2+}Y zeolite by the same procedure shown in Scheme 2. Diffuse reflectance spectra (Fig. 2) revealed that within hydrated Ca^{2+} Y zeolites the thionin molecules exist as dimers. When this sample was partially dehydrated on a vacuum line at room temperature

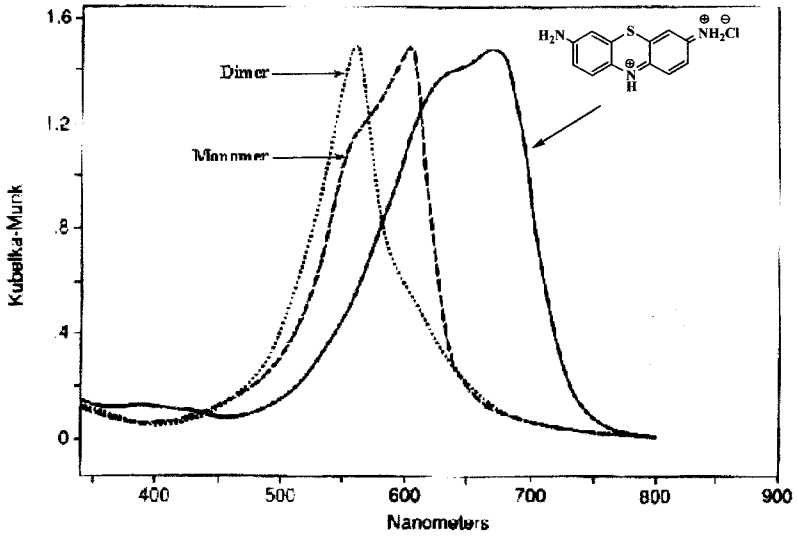

Figure 2. Thionin included in CaY under wet (dimer), dry (monomer) and very dry (protonated from) conditions.

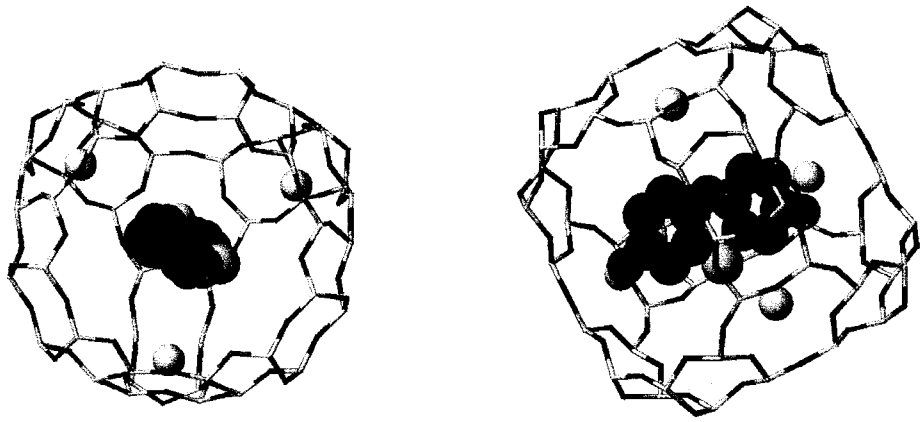

Figure 3. Two views of the possible location of thionin within the supercage of NaY zeolite. Picture has been generated using CAChe program based on the methylene blue–NaY structure reported in Ref. 17. Three Na^+ ions are also shown in the cage. Thionin is at the center of the cage with one of the NH_2 groups projecting itself towards the adjacent cage via the 7.4 Å window.

the color changed from pink to blue and the diffuse reflectance spectrum was that of the monomer. When the sample was further dried by degassing (10^{-4} mm) at ~100°C, the sample turned to a green color. The red shifted diffuse reflectance spectrum (λ_{max}=672 nm) is identified as that of *protonated* thionin.[14] It is known that the dehydration of divalent ion exchanged X and Y zeolites results in dissociation of water molecules to generate free protons.[15] It has also been established that the generation of protons is related to the polarizing power of the cation; the larger cation Ba^{2+} has no ability to dissociate water. Indeed, thionin was protonated, as evidenced by spectral changes, only in Mg^{2+}, Ca^{2+}, and Sr^{2+}Y and not in Ba^{2+}Y. The above complication due to protonation was also observed in the case of methylene blue and methylene green. Because of the Brønsted acidity problems, M^{2+}Y zeolites were not employed in this oxidation study.

In the context of spectral hole burning, thionin and methylene blue included NaY zeolite have attracted considerable attention from the groups of Schulz-Ekloff and Deeg.[16] Schulz-Ekloff and co-workers have characterized the methylene blue-NaY samples by X-ray photoelectron spectroscopy and X-ray powder diffraction (by Rietveld refinement). On the basis of X-ray powder diffraction they believe that the cation exchanged methylene blue molecule remains at the centers of the supercages of NaY.[17] Since our loading level as well as the method of preparation are similar to that of Schulz-Ekloff we assume that even in our samples the dye molecules are uniformly distributed and remain at the centers of the supercages. Based on the above results of Schulz-Ekloff and co-workers[17] a model for thionin included in NaY generated with the CAChe program is provided in Fig. 3.

Generation of singlet oxygen

Excitation of thionin, methylene blue and methylene green exchanged NaY zeolites as prepared (wet) did not show any emission. It is known that the dimeric forms of the above dyes do not emit.[18] However, excitation of the 'dry' samples of dye exchanged NaY emitted fluorescence characteristic of the monomeric dye. In addition to the fluorescence from the dye, oxygen saturated 'dry' samples showed an emission (1268 nm) attributable to singlet oxygen.[19] The intensity of the emission varied from sample to sample and was very sensitive to the water content of the sample. We had difficulties in observing emission from samples stored over a week. The 1268 nm emission suggested to us that singlet oxygen is generated within zeolites by the sensitization process. This was confirmed through 'chemical tests' by isolating products characteristic of singlet oxygen oxidation of olefins such as 2,3-dimethyl-2-butene (**1**), 2,4,4-trimethyl-2-pentene (**3**) and 1,2-dimethylcyclohexene (**5**) (Schemes 3 and 4).[20]

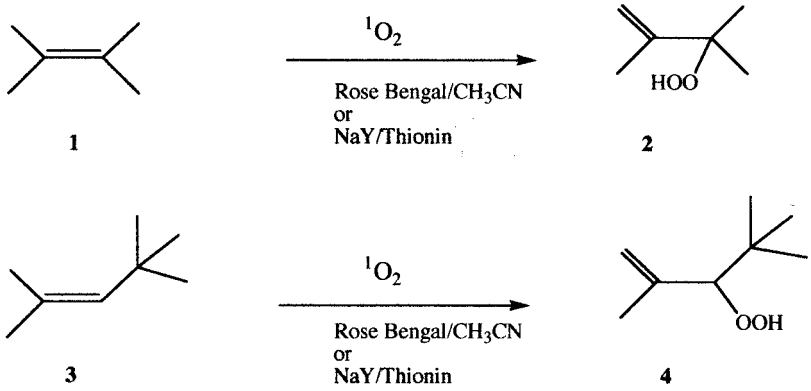

Scheme 3.

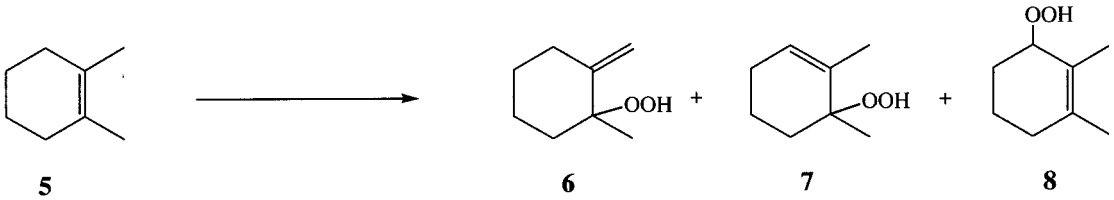

Rose Bengal / Acetonitrile	89	11	0
Thionin / Na Y/Hexane	90	10	0
Autooxidation	6	39	54

Scheme 4.

The experimental protocol adopted to achieve oxidation of alkenes within zeolites is outlined in Scheme 2. Since methylene blue and methylene green included zeolites gave results similar to thionin we present the results obtained with thionin exchanged zeolites only. The pink thionin–NaY sample (300 mg) was dried in an air oven at 120°C for 24 h by which time the sample turned blue. The 'dry' thionin–NaY sample was added to a dry hexane solution (12 mL) containing the alkene (12 μL) of interest. The mixture was stirred, bubbled with oxygen and irradiated with a 450 W medium pressure mercury lamp fitted with a Corning filter CS #3.73 (>420 nm). The blue zeolite slurry at the beginning of the irradiation turned grey following about 3 h of irradiation. The slurry was filtered and the hexane filtrate was analyzed for products and unreacted alkene by GC. The hydroperoxide products from the zeolite residue were extracted by stirring the residue with either acetonitrile or tetrahydrofuran–water (5%) mixture for about 12 h. To the extract excess triphenyl phosphine was added with stirring. Upon addition of triphenyl phosphine the product hydroperoxides were converted to the corresponding alcohols. The allylic alcohols thus generated from the hydroperoxides were analyzed by GC. The vacuum (2×10^{-3} mm, 60°C) as well as oven (120°C, 24 h) dried samples gave similar results. Due to the less tedious process of drying in an air oven at 120°C as compared to drying on a vacuum line, the former procedure was generally adopted for all oxidation studies.

Irradiation of the dye exchanged zeolite in the presence of 2,3-dimethyl-2-butene (**1**) gave the same hydroperoxide (**2**) as in isotropic media (solution irradiations were carried out in acetonitrile using rose bengal as the sensitizer).[20] Irradiation of 2,4,4-trimethyl-2-pentene (**3**) under the same conditions gave the expected hydroperoxide (**4**) as well (Scheme 3). These results demonstrate that not only is singlet oxygen generated within the zeolites, it is was reactive as well. Further confirming the fact that the hydroperoxides we observe are obtained via the ene reaction due to the generation of singlet oxygen and not via other pathways are the results obtained with 1,2-dimethylcyclohexene (**5**).[20a] It has been shown previously that singlet oxygen and autoxidation via a radical pathway yield a different distribution of products (Scheme 4).[20a,8] As is evident from Scheme 4, the product distribution in zeolites corresponds to oxidation via the singlet oxygen pathway.

Regioselective hydroperoxidation of 2-methyl-2-heptene and 1-methylcyclooctene

Having established that generation of singlet oxygen within a zeolite is feasible, we proceeded to investigate the

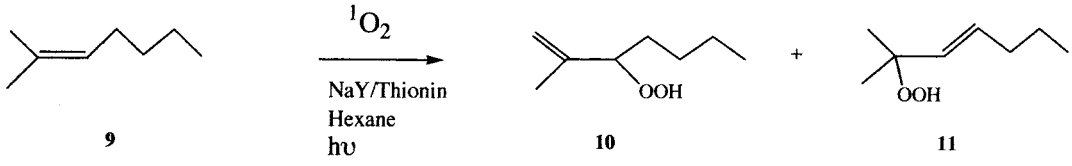

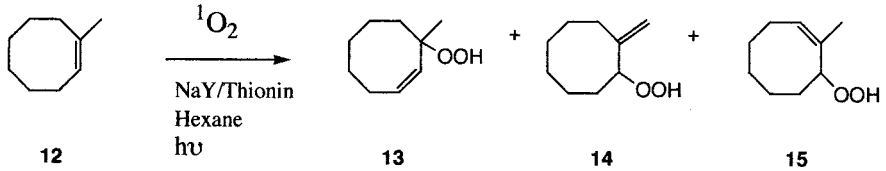

Scheme 5.

Table 1. Photooxidation of 2-methyl-2-heptene (an average of six runs is provided with an error limit of ±3%)

Medium	Time of irradiation	Relative ratio[a] **11:10**	Conversion (%)[b]	Mass balance (%)[c]	Corrected ratio[d]
CH_3CN/Rose bengal	30 min	51:49	75	94	
LiY/Thionin	15 min	19:81	22	92	26:74
NaY/Thionin	15 min	21:79	22	94	26:74
KY/Thionin	15 min	25:75	21	86	36:64
RbY/Thionin	15 min	30:70	20	84	41:59
CsY/Thionin	15 min	38:62	21	80	50:50
LiY/Thionin	3 h	05:95	69	46	
NaY/Thionin	3 h	11:89	63	65	
KY/Thionin	3 h	22:78	62	78	
RbY/Thionin	3 h	26:74	60	58	
CsY/Thionin	3 h	30:70	60	50	
NaY/Thionin	15 min	21:79	22	94	
NaY/Thionin	30 min	20:80	28	89	
NaY/Thionin	45 min	18:82	34	84	
NaY/Thionin	1 h	16:84	43	74	
NaY/Thionin	3 h	11:89	63	65	
NaY/Thionin	6 h	00:100	65	52	

[a] The alcohols were analyzed by GC (obtained by converting the peroxides of 2-methyl-2-heptene using PPh_3).
[b] Percentage conversion based on the amount of recovered 2-methyl-2-heptene.
[c] Mass balance calculated from recovered alcohols and 2-methyl-2-heptene.
[d] Assuming the decrease in mass balance is due only to the decompositon of hydroperoxide **11**.

regioselectivity during the oxidation of two olefins, 2-methyl-2-heptene (**9**) and 1-methylcyclooctene (**12**). In the case of **9** two hydroperoxides **10** and **11** (Scheme 5) and in the case of **12** three hydroperoxides **13**–**15** are expected (Scheme 5).[21] For comparison with isotropic solution media, reactions were performed in acetonitrile using rose bengal and thionin as sensitizers. The products obtained were consistent with literature reports.

The experimental procedure adopted for sample preparation, irradiation, isolation and analyses of products is the same as that described above in the case of alkenes **1**, **3** and **5** (Scheme 2). A typical slurry used for irradiation consisted of 12 mL of hexane, 250 mg of dry thionin–M^+Y zeolite and 12 μL of alkene. The oxidation products were characterized by ^1H NMR and by comparison with authentic samples prepared by solution irradiation and analyzed by GC. The recovery (mass balance) was estimated by GC using undecane as the calibration standard. The results obtained for short (10–15 min) and long (3 h) irradiation times in the case of 2-methyl-2-heptene and 1-methylcyclooctene are provided in Tables 1 and 2, respectively. On perusal of Table 1 it is evident that the ratios of the two peroxides **11** to **10** from 2-methyl-2-heptene within LiY and NaY depended on the duration of irradiation, longer irradiation favoring the secondary hydroperoxide **10**. At longer irradiation times, the mass balance decreases. A similar change in product distribution was also seen in the case of 1-methylcyclooctene (Table 2). More importantly, in both cases (Tables 1 and 2) while the recovery (mass balance) was near 90% with short duration of irradiation, the longer irradiation resulted in a poor recovery (<50%).

Table 2. Results of oxidation of 1-methylcyclooctene (an average of six runs is provided with an error limit of ±3%)

Medium	Time of irradiation	Relative ratio[a]			Conversion (%)[b]	Mass balance (%)[c]	Corrected ratio of **14:(13+15)**[d]
		13	**14**	**15**			
Methanol[e]		31	27	42	–	–	
Rose bengal/CH_3CN	45 min	21	29	50	–	–	29:71
LiY/Thionin	10 min	5	65	30	27	92	60:40
NaY/Thionin	10 min	6	76	18	52	80	61:39
KY/Thionin	10 min	15	62	23	53	80	50:50
RbY/Thionin	10 min	18	60	22	38	94	56:44
CsY/Thionin	10 min	15	55	30	22	89	49:51
LiY/Thionin	3 h	1	80	19	99	20	
NaY/Thionin	3 h	6	65	29	98	23	
KY/Thionin	3 h	21	75	4	93	41	
RbY/Thionin	3 h	19	60	21	76	39	
CsY/Thionin	3 h	22	39	39	72	53	

[a] Relative ratios were estimated using relative areas of the three alcohols in the GC trace.
[b] Percentage conversion refers to the reacted 1-methylcyclooctene.
[c] Percentage mass balance refers to the total of the unreacted 1-methylcyclooctene and the three alcohols.
[d] Corrected ratio of **14:(13+15)** accounts for all lost products into **(13+15)**.
[e] Foote, C. S. *Pure Appl. Chem.* **1971**, *27*, 635.

The low mass balance with longer irradiation suggests that the product distributions obtained following 3 h of irradiation may not reflect the primary oxidation process. On the other hand, considering the high recovery, the distributions obtained following 10–15 min of irradiation are more likely to be meaningful. Clearly, following 10–15 min of irradiation there is significant regioselectivity in the product hydroperoxides. While in solution, 2-methyl-2-heptene **9** yields the two hydroperoxides **10** and **11** in equal amounts, within LiY and NaY the secondary hydroperoxide **10** is favored (Table 1). Similarly, zeolites favor the *exo*-methylene hydroperoxide **14** in the case of 1-methylcyclooctene **12** (Table 2). To examine whether selective loss of **11** in the case of 2-methyl-2-heptene and **13** and **15** in the case of 1-methylcyclooctene would account for the observed selectivity, the product distributions were recalculated assuming that all the alkene that is not accounted for (i.e. 100% mass balance) is due to the loss of **11** in the case of 2-methyl-2-heptene and **13** and **15** in the case of 1-methylcyclooctene. The recalculated numbers for the two alkenes are provided in the last column of Tables 1 and 2. These numbers also suggest that the oxidation within a zeolite occurs with moderate regioselectivity. Based on the data provided in Tables 1 and 2 we believe that there is selectivity towards **10** in the case of 2-methyl-2-heptene and **14** in the case of 1-methylcyclooctene. The observed regioselectivity depends on the M^+ ion. Generally Li^+ and Na^+ ions give higher selectivity while Cs^+ gives lower selectivity. It may be noted that identical regioselectivities were obtained within zeolites when either methylene blue or methylene green was used as a sensitizer (to conserve space data are not included).

A point to note is that only 10% of the alkene remained inside the zeolite (one molecule per 15 supercages), with most of the alkene staying in the hexane layer. On the other hand, the product hydroperoxide prefers the zeolite surface over the hexane solvent. GC analyses at the end of the oxidation detected no hydroperoxide in the hexane layer. The presence of a polar group with lone pairs of electrons (OOH) seems to aid in anchoring the hydroperoxide within the zeolite.

The following experiment suggested that, in spite of most of the alkene remaining in the hexane, the regioselective oxidation during sensitization by thionin occurs within the zeolite. In one set of experiments, tetraphenyl porphyrin (TPP), a molecule too large to be included within NaY, was adsorbed on the outside surface of the activated (500°C, oven) NaY and used as the sensitizer. When a hexane slurry of 2-methyl-2-heptene and TPP-NaY was irradiated with continuous purging of oxygen for 30 min the two peroxides **10** and **11** were obtained in equal amounts. We interpret this observation to indicate that the singlet oxygen generated on the exterior surface of the zeolite reacts with the alkene present in the hexane layer resulting in no selectivity. This control experiment supports the view that the singlet oxygen generated within a zeolite by using sensitizers small enough to be included within the supercages of a Y zeolite, reacts with alkenes adsorbed within the zeolite with a regioselectivity different from that which occurs in the hexane layer.

Table 3. Stability of peroxides of 2-methyl-2-heptene inside zeolite—3 h irradiation (the peroxides were found to decompose in NaY/Thionin when stirred in dark for 3 h with 66% mass balance and relative ratio of **11:10**=18:82; the peroxides were stable in NaY; an average of six runs is provided with an error limit of ±3%)

Zeolite	Relative ratio after irradiation[a,b] **11:10**	Mass balance (%)[c]
LiY/Thionin	05:95	46
NaY/Thionin	13:87	65
KY/Thionin	34:66	68
RbY/Thionin	38:62	58
CsY/Thionin	42:58	50

[a] Initial ratio of **11:10**=45:55.
[b] The peroxides were analyzed as alcohols by GC before and after irradiation.
[c] Mass balance calculated based on the recovered alcohols.

Complications due to poor stability of product hydroperoxides to light and oxygen

The dependence of the ratio of the product hydroperoxides and the mass balance on the duration of irradiation (Tables 3 and 4) suggested to us that the oxidation products may be unstable towards singlet oxygen generated during irradiation of the dye. To check the stability of hydroperoxides under irradiation conditions in the thionin–NaY zeolite slurry, the two peroxides **10** and **11** from 2-methyl-2-heptene and three peroxides **13–15** from 1-methylcyclooctene were synthesized by solution irradiation. The two hydroperoxides **10** and **11** from 2-methyl-2-heptene obtained in the ratio 55:45 by solution irradiation were

Table 4. Stability of the hydroperoxides of 1-methylcyclooctene inside zeolite—3 h irradiation (an average of six runs is provided with an error limit of ±3%)

Zeolite	Conditions	Relative ratio after irradiaton[a,b] **13:14:15**	Mass balance (%)[c]
LiY	No ($h\nu$, O_2/N_2)	0:42:58	62
NaY		16:38:46	85
KY		21:33:46	77
RbY		21:34:45	96
CsY		22:32:46	86
LiY	$h\nu$, O_2	16:35:49	89
NaY		21:30:49	89
KY		21:31:48	87
RbY		22:30:48	76
CsY		21:30:49	78
LiY/Thionin	$h\nu$, O_2	1:93:6	24
NaY/Thionin		35:65:0	34
KY/Thionin		47:53:0	33
RbY/Thionin		36:56:8	45
CsY/Thionin		21:36:43	74
LiY/Thionin	$h\nu$, N_2	0:28:72	42
NaY/Thionin		19:40:41	37
KY/Thionin		24:38:38	27
RbY/Thionin		20:35:45	36
CsY/Thionin		21:33:46	21

[a] Initial ratio of **13:14:15**=21:29:50.
[b] The peroxides were analyzed as alcohols by GC before and after irradiation.
[c] Mass balance calculated based on the recovered alcohols.

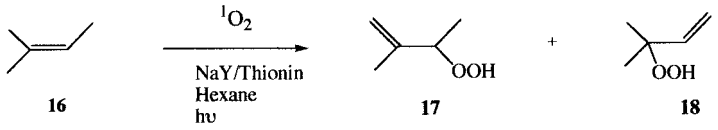

thionin/acetonitrile	51	49
thionin/NaY	72	28

Scheme 6.

introduced into the thionin–NaY zeolite and irradiated as a hexane slurry (GC analysis of the hexane ensured that the two hydroperoxides were completely adsorbed within the zeolite). Following three hours of irradiation under conditions identical to alkene oxidation, the products were extracted as hydroperoxides and analyzed as alcohols (after addition of triphenyl phosphine) by GC. The final ratio and the mass balance are provided in Table 3. The tertiary peroxide **11** is selectively lost in this process. Several new peaks that appeared on the GC trace were not characterized. While the selective loss was observed in LiY and NaY, in KY, RbY and CsY the two peroxides were lost to the same degree. The initial ratio of the three peroxides **13**–**15** from 1-methylcyclooctene was 21:29:50. As shown in Table 4, irradiation under oxygen saturated conditions caused the ratio to change in favor of the *exo*-methylene hydroperoxide **14**. The light-instability of the peroxides was independent of the dye used (data not shown). Further, the peroxides were stable within dye exchanged zeolites in the absence of irradiation, and upon irradiation under nitrogen saturated conditions, all three hydroperoxides were lost to the same extent indicating the necessity of dye and light. As seen in Table 4, upon irradiation of the three hydroperoxides included in dye exchanged NaY, **15** is selectively destroyed indicating the necessity of oxygen.

We believe that one of the pathways by which the hydroperoxides are destroyed within a zeolite involves singlet oxygen. It is not surprising that the hydroperoxides, which also contain a reactive olefinic group, react with singlet oxygen in a manner similar to the parent alkene. The reactivity of the hydroperoxides towards singlet oxygen is expected to depend on the electron richness of the C=C bond. For exampe, compound **11**, which contains an internal C=C bond, would be expected to react at a higher rate than compound **10** with singlet oxygen. Similar reasoning would lead one to conclude that the reactivity order in the case of hydroperoxides from **12** would be **15**>**13**>**14**. Loss of **11** in the case of alkene **9** and **15** in the case of alkene **12** is consistent with this hypothesis.

A factor favoring secondary oxidation of hydroperoxides is their preference to stay within a zeolite. Between the product peroxides and the reactant olefin the former would be expected to stay within a zeolite. Such a preference would favor the secondary oxidation of the product hydroperoxide. This relative increase in secondary oxidation is expected to lead to the selective accumulation of the least reactive hydroperoxides **10** and **14**. If the above reasoning is correct, 2-methyl-2-butene **16** would be expected to give a time independent product distribution (Scheme 6). In this case both hydroperoxides **17** and **18** are unlikely to undergo secondary oxidation. As expected, irradiation of **16** within thionin–NaY gave **17** and **18** in the ratio 72:28 that remained constant from 15 min to 3 h of irradiation. Due to the volatility of the alkene, the mass

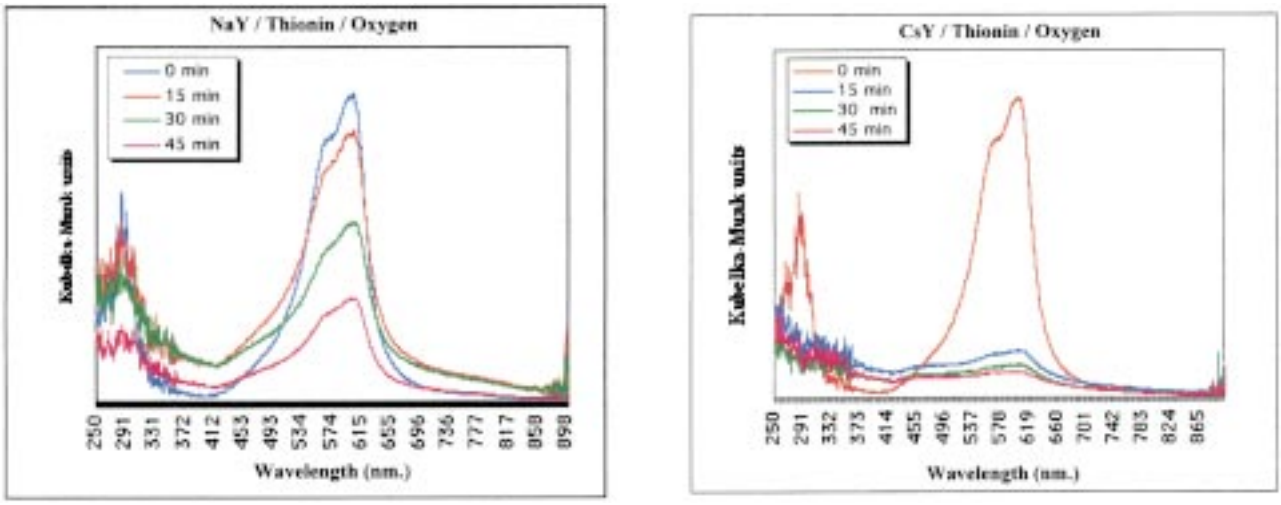

Figure 4. The diffuse reflectance spectra of thionin in NaY (left) and thionin in CsY (right) following irradiation for the given time on the insert. The top spectrum in each one corresponds to time zero and the bottom to 45 min of irradiation.

balance, could not be estimated accurately. It is also of interest to note that the 72:28 ratio is close to the number that we obtained in the case of 2-methyl-2-heptene for 15 min of irradiation within thionin–NaY.

Complications due to poor stability of the dyes to light and oxygen

Comparison of the product distributions in relation to the duration of irradiation within NaY and CsY zeolites provided further insight into the oxidation process. Perusal of Tables 1 and 2 indicates that under photolysis conditions the hydroperoxides were less stable within NaY than in CsY. This was especially noticeable in the case of the hydroperoxides from **12**. For example, the mass balance in the case of **12** within LiY decreased from 92% for 10 min of irradiation to 20% for 3 h of irradiation (Table 2). Within CsY the change was less (89–53%, Table 2). This suggested to us that the dye-induced decomposition of the hydroperoxides occurs less readily within CsY. We therefore examined the photostability of dyes included within M^+Y zeolites. The dyes were found to be less stable within CsY than in NaY. The photostabilities of the three dyes, thionin, methylene blue and methylene green within NaY and CsY were monitored by their diffuse reflectance spectra. Spectral changes in the case of thionin are shown in Fig. 4 (the other two dyes exhibited similar behavior). When thionin included NaY and CsY zeolites were irradiated under the same conditions used for the oxidation of alkenes, the dye decomposed and the absorption band in the visible region was lost. The extent of decomposition varied with the cation. All three dyes within NaY decomposed by less than 25% after 15 min of irradiation, whereas within CsY more than 60% of the dyes had decomposed for the same time. No attempt was made to isolate the products of the decomposition of the dyes. The dyes most likely decompose via an electron transfer pathway in which the zeolite acts as a donor.[22] Thionin and related dyes in their excited states have been established to accept electrons from suitable donors. It has also been shown that the zeolite surface can serve as an electron donor.[23] Further it has been established that CsY is a better electron donor than NaY.[23] Our observation of the dye being less stable within CsY than in NaY is consistent with these established facts.

We believe that the stability of the hydroperoxides within CsY results from the absence of generation of singlet oxygen on complete decomposition of the dye which occurs within 30 min of irradiation. On the other hand, the more stable dyes within NaY continue to generate singlet oxygen for a longer time. Thus the difference in singlet oxygen generation, we believe, accounts for the difference in stability of the hydroperoxides within NaY and CsY. It may be noted that the above three dyes were more stable when they were irradiated in the presence of nitrogen.

Complications due to Brønsted acid sites

A comparison of the behavior of *para*-1-menthene (**21**) and limonene (**22**) and the olefins **19** and **20** illustrates the point. While *para*-1-menthene reacted cleanly within a zeolite, limonene gave a complex mixture (Schemes 7 and 8). Similarly, while the trisubstituted olefin **19** was well behaved, the analogous trisubstituted olefin **20** underwent geometric isomerization and rearrangement even before the initiation of the oxidation (Scheme 7). Thus the olefins are thermally reactive within zeolites.

For mechanistic studies we were interested in carrying out the oxidation of pure *Z* and *E* isomers of 6-methyl-6-dodecene, 5-methyl-5-decene and 3-methyl-3-hexene. To our great disappointment, stirring the pure isomers of these alkenes with thionin–NaY for about 15 min (without light) resulted in geometric isomerization yielding 1:1 mixtures of *E* and *Z* isomers. To minimize this unwanted reaction we used zeolites from several sources such as Aldrich, PQ corporation (CBV-100), Englehard (EZ-150) and Union carbide (LZY-52) and all were found to bring about the above thermal isomerization process. Similarly, when 2-carene, 3-carene, α-pinene and limonene were stirred with thionin–NaY, they all rearranged to yield a number of products (not characterized). It is important to note that olefins **1**, **3**, **5**, **9**, **12**, and **16**, whose oxidation chemistry was described in previous sections, were thermally stable within

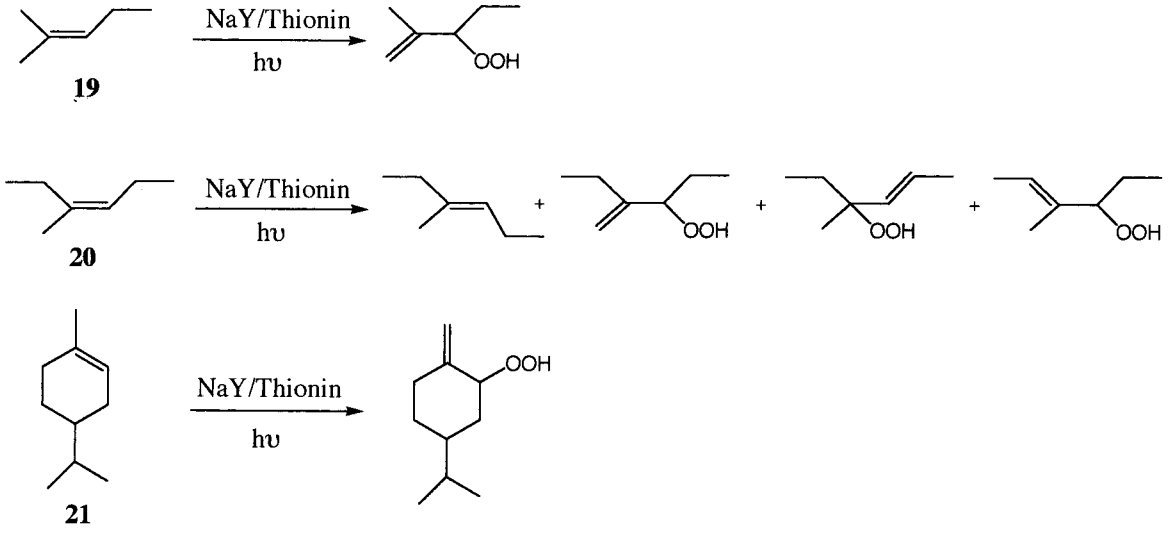

Scheme 7.

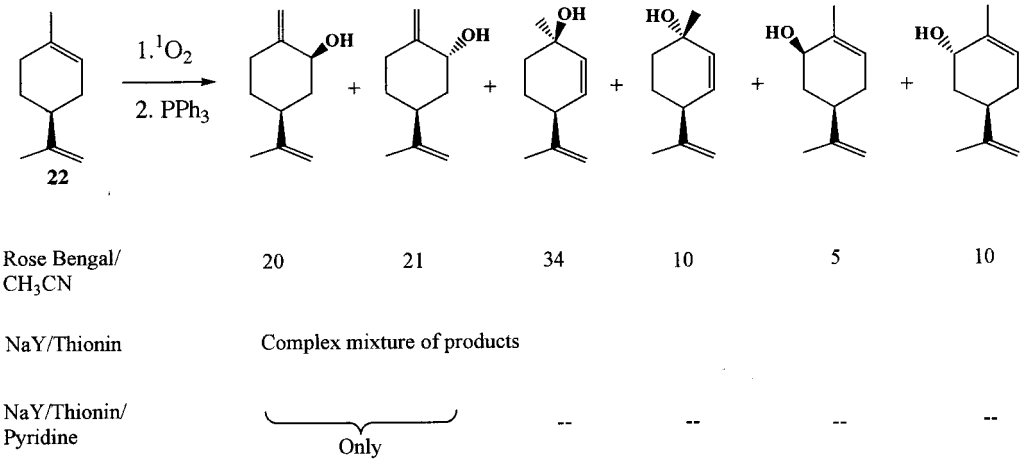

Scheme 8.

thionin–NaY. No new peaks were detected and the original alkenes were quantitatively isolated following stirring with thionin–NaY. We believe the side reactions observed with 2-carene, 3-carene, α-pinene and limonene can be understood on the basis of Brønsted acid chemistry.

When the present study was initiated not much attention was paid to the potential acidic nature of NaY. Based on the complications we encountered, we felt that it was important to establish the presence of Brønsted acid sites within NaY, estimate the number of acidic sites present and find a way to inactive the zeolite. By using an 'indicator method' employing retinol as an indicator we have characterized NaY from Aldrich, PQ corporation (CBV-100), Englehard (EZ-150) and Union carbide (LZY-52) to be mildly acidic and estimated to contain one Brønsted acid site per two unit cells.[24] The oxidation process is generally not influenced by the presence of such a small number of acidic sites. However, when the protonated alkene undergoes other reactions, the products of oxidation become complex. Under such conditions, the acid sites can act as a catalyst and effect isomerization of an alkene from a thermodynamically less stable to a more stable isomer.

If the above analysis is correct, olefins that are susceptible to cationic rearrangements are expected to yield a complex mixture of products during oxidation unless the acidity of NaY–thionin can be controlled. A conventional acid–base chemistry approach has led to such control. In order to avoid acid catalyzed side reactions NaY–thionin was doped with a controlled amount of a base such as pyridine or diethyl amine. The experiment consisted of stirring the activated NaY–thionin in hexane and adding a known amount of a base (pyridine or diethyl amine) that is required to quench the acidic sites (~one acid site in 16 supercages). The mixture was stirred for at least 5 h and the olefin added and irradiated. The results obtained in the case of limonene are shown in Scheme 8.[20b] Clearly the problem of rearrangement was solved by this approach. It is important not to overload the zeolite with a base since the latter, when present in excess, displaces the olefin to the hexane layer. We have found pyridine to be a better base in the context of oxidation; diethyl amine displaces the olefin to the hexane layer or yields a complex mixture of products or completely quenches the oxidation process.

Theoretical studies on metal–olefin complexes

After correcting for all the complicating factors that influence the observed product distributions, there is still a marked regioselectivity in the hydroperoxidation of trisubstituted alkenes within zeolites which is cation dependent. Formation of the secondary hydroperoxide (**10**) derived through hydrogen abstraction from the gem-dimethyl groups of **9** is clearly favored with Li^+ and Na^+ containing zeolites. The preference becomes progressively less with the heavier alkali metal ions. For the reaction involving 1-methylcyclooctene (**12**), the hydroperoxide containing an *exo*-methylene unit (**14**) is the predominant product. Again, the selectivity is significantly reduced in the Cs^+ exchanged zeolite. In order to obtain more insights on the role of cations on the observed product distributions, ab initio and DFT calculations were carried out on model systems. In view of the complexities involved in the reactions inside the zeolite cage, the goals of the computational work were necessarily limited to a few specific aspects. First, the magnitude of the interaction energies between various cations and representative olefins were quantified. These provide a measure of the potential role of different cations in altering the reactivity patterns of the olefins with singlet oxygen. In addition to the energies, unsymmetrical distortions in the optimized geometries as well as frontier orbitals were analyzed. In the next step, the effect of metal coordination on the transition state for hydrogen abstraction was explicitly examined.

The geometries of olefins coordinated to different metal cations, Li^+, Na^+, K^+, Rb^+, Cs^+, Ba^{++}, Sr^{++}, were optimized at the Hartree–Fock (HF), second order Mollet–Plesset theory (MP2) and hybrid Hartree–Fock and Density Functional method (B3LYP).[25] The 6-31G** basis set including polarization functions on all atoms (d for heavy atoms, p for hydrogens) was employed for all calculations.[26] For the heavier elements, K, Rb, Cs, Ba and Cs, Hay–Wadt Effective Core Potentials (ECP) including relativistic corrections were used.[27] The computed interaction energies,

Table 5. Calculated interaction energies (kcal mol^{-1}) between metal cations and alkenes at three theoretical levels

Metal ion	Olefin	HF	MP2	B3LYP
Li^+	Ethylene	−23	−24.3	−24.9
	Propene	−25.5	−27.1	−28.2
	Isobutene	−26.4	−28.8	−29.6
	Trimethylethylene	−27.6	−30.6	−31.3
Na^+	Ethylene	−15.8	−16.8	−17.8
	Propene	−17.2	−18.6	−19.9
	Isobutene	−17.7	−19.6	−20.6
	Trimethylethylene	−18.3	−20.6	−21.5
K^+	Ethylene	−7.7	−8.5	−8.8
	Propene	−7.9	−9.8	−10
	Isobutene	−9.6	−10.9	−11.2
	Trimethylethylene	−9.5	−11.6	−11.1
Rb^+	Ethylene	−6.4	−7.2	−7.2
	Propene	−6.4	−8.3	−8.3
	Isobutene	−7.8	−9.2	−9.1
	Trimethylethylene	−7.7	−9.9	−8.9
Cs^+	Ethylene	−4.7	−5.4	−5
	Propene	−4.5	−6.4	−5.9
	Isobutene	−5.8	−7.1	−6.6
	Trimethylethylene	−5.8	−7.8	−6.4
Sr^{++}	Ethylene	−27.4	−28.8	−32.5
	Propene	−35.1	−36	−42.2
	Isobutene	−40.9	−42	−49.1
	Trimethylethylene	−41.6	−46.7	−51
Ba^{++}	Ethylene	−21.9	−23.5	−26.5
	Propene	−27.5	−29.5	−34.5
	Isobutene	−32.5	−34.5	−40.2
	Trimethylethylene	−33.7	−37.7	−42.7

without corrections for basis set superposition errors as well as zero point and thermal energy terms, are provided in Table 5.

The binding energies confirm the magnitude of cation–π interactions quantified in earlier experimental[28] and theoretical[29] studies on a few systems. As expected, the strength of the interaction is relatively large for Li^+ and Na^+ and becomes progressively smaller for the heavier alkali metal cations. The Cs^+ complex is very weakly bound. In view of their enhanced charge, Ba^{++} and Sr^{++} are calculated to have binding energies which are quite substantial. Introduction of methyl substituents enhances the magnitude of interaction, although the increase is relatively modest.

Within a zeolite, the cations are bound to oxygen counterions. As a result, the metal ions are likely to interact less effectively than usual with an olefin. Nevertheless, the trends in the relative binding energies are expected to be similar to those computed for the free cations. Of the cations examined, Li^+, Na^+, Sr^{++} and Ba^{++} are predicted to have the strongest interaction with alkenes. However, the strength of metal binding to benzene is substantially higher. These ions are expected to favor the adsorption of alkenes within the zeolites, although to a lesser extent than aryl systems.

The complex of trimethylethylene (2-methyl-2-butene; TME) is the model most closely resembling the systems examined experimentally. The computed structure of the lithium complex is shown in Fig. 5. The metal cation is not directly above the π bond, but is displaced. The unsymmetrical disposition of the metal is even more pronounced at the MP2 level, with the metal quite significantly displaced towards one of the methyl groups (note the distance $Li–C_1$ and $Li–C_5$ in Fig. 5). Such attractive interactions between Li^+ and alkyl groups have been noted earlier through calculations and analysis of crystal structures.[30] The distortions become less for the heavier alkali metal complexes. The optimized geometry of the Cs^+ complex is shown for comparison in Fig. 5. This geometric effect may have implications for the preferred conformation of the perepoxy intermediate formed by reaction of the metal–olefin complex with singlet oxygen and may in turn determine the preferred site of hydrogen abstraction.

Even in the less distorted structure obtained at the

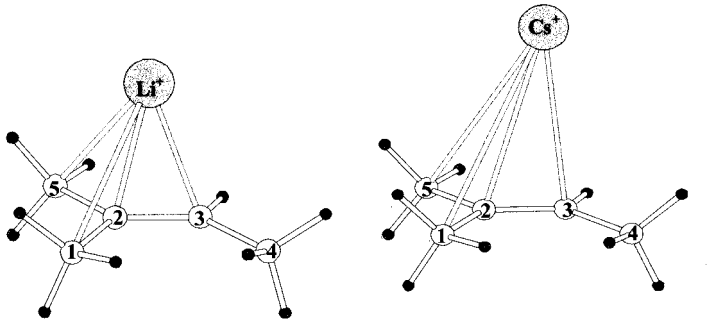

	Li-C3	Li-C2	Li-C1	Li-C5	Cs-C3	Cs-C2	Cs-C1	Cs-C5
HF	2.27	2.49	3.32	3.15	3.74	3.85	4.38	4.33
MP2	2.33	2.27	3.32	2.41	3.58	3.64	4.13	4.15
B3LYP	2.31	2.24	3.28	2.39	3.60	3.76	4.32	4.28

Figure 5. Calculated key metal–carbon distances (Å) in Li^+ and Cs^+ complexes of trimethylethylene.

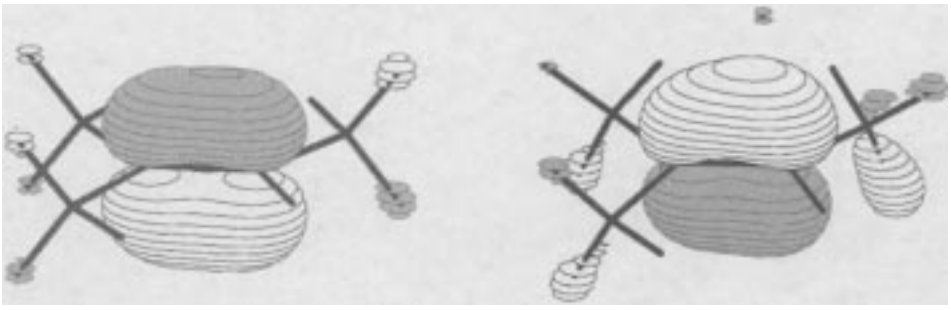

Figure 6. The π HOMO of 2-methyl-2-butene (left) and its Li^+ complex (right) calculated at the HF/6-31G** level.

HF/6-31G** level, an interesting orbital polarization is seen. Since the oxidation process is initiated by electrophilic attack at the olefin, the key orbital is the HOMO of the alkene.[31] The π HOMO of TME and its Li^+ complex are shown in Fig. 6. Several interesting changes are noticeable on complexation. The π lobes are, as expected, polarized towards the metal. The lobes are also relatively larger on the less substituted olefin center. Hence, the preferred site of initial attack of singlet oxygen may be the corresponding carbon atom. Consequently, hydrogen abstraction is likely to be favored from one or both of the gem-dimethyl groups. However, another interesting polarization is seen in Fig. 6. The repulsive interaction between the π MO and the C–H sigma orbital is more pronounced in the complex. This is understandable since the π MO would be lowered in energy due to metal coordination bringing it closer to the filled sigma orbitals. The coefficient at the hydrogen atom pointing away from the metal is clearly larger. The polarization is significant on the mono-methyl group. This leads to the conclusion that hydrogen abstraction from the mono-methyl group would lead to greater stabilization at the cyclic transition state for the ene reaction.

Since ground state effects do not provide a clear clue to the preferred site of hydrogen abstraction, precise transition state calculations were carried out. The potential energy surfaces for the [2+2] cycloaddition and ene reaction of simple olefins with singlet oxygen have been extensively investigated using various theoretical methods.[32] While the results are quite sensitive to the level of theory employed, a 1,4-biradical, the corresponding zwitterion and the perepoxy species, have been implicated as key intermediates. The preferred pathway has been suggested to be dependent on the nature of substituents and solvent. The question of regioselectivity in hydroperoxidation of unsymmetrical olefins has also been addressed in a few studies. In particular, the relative barriers for the formation of secondary and tertiary hydroperoxides from trimethylethylene have been computed, although the distinction between hydrogen abstraction from the *syn* and *anti* methyl groups has not been made. In the present study, we focussed on the three possible transition states for the hydrogen abstraction step in the ene reaction of trimethylethylene and examined the effect of lithium coordination on the nature of these structures.

Transition state structures were optimized at the HF/6-31G** level and characterized to have a single imaginary vibrational frequency corresponding to the hydrogen abstraction process. In each regioisomeric structure, one C–O bond is nearly completely formed (C3–O4, Table 6) and the migrating hydrogen is more closely bound to the carbon than to the oxygen atom (C1–H6 and O5–H6). The structures correspond to transition states for hydrogen migration from the 1,4-biradical intermediates. To obtain accurate energetics, zero point energies, thermal corrections as well as the entropy of activation were then computed. To include electron correlation effects in these structures with significant biradical character, additional calculations were carried out at the MP2 and B3LYP levels. The corresponding activation energies and free energies of activation (at 298 K) are provided in Table 7. As noted in earlier high

Table 6. Optimized values of key geometric parameters (distances in Å; angles in degrees. Atom numbering is shown below) in the transition states for hydrogen abstraction from trimethylethylene (TME) and its lithium complex by $^1O_2$

Parameter	$TME+{}^1O_2$			$Li^+\cdots TME+{}^1O_2$		
	R1 R2 R3 Me H Me	R1 R2 R3 Me Me H	R1 R2 R3 H Me Me	R1 R2 R3 Me H Me	R1 R2 R3 Me Me H	R1 R2 R3 H Me Me
C3–O4	1.414	1.421	1.435	1.902	1.861	1.9
O4–O5	1.391	1.39	1.379	1.245	1.249	1.242
O5–H6	1.507	1.5	1.462	1.326	1.357	1.322
H6–C1	1.205	1.206	1.233	1.263	1.257	1.268
C1–C2	1.425	1.423	1.415	1.436	1.431	1.431
C2–C3	1.476	1.477	1.473	1.396	1.399	1.405
Li–C1	–	–	–	2.394	2.488	2.508
Li–C2	–	–	–	2.308	2.304	2.461
Li–C3	–	–	–	2.907	2.575	3.055
C2–C3–O4	84.8	84.7	81.2	90.3	90.7	86.9
C3–O4–H5	111.4	113	114.5	115.1	113.7	114.7
O4–O5–H6	91.4	91.9	92.1	105.1	104.6	104.9
C1–C2–C3	116	118.7	122.4	115.7	117.8	121.7

Table 7. Calculated activation energies and free energies (kcal mol^{-1}) for hydrogen abstraction from trimethylethylene(TME) and its lithium complex by singlet oxygen (transition state structures have been optimized at the HF/6-31G**//HF/6-31G** level. Activation energies include zero point and thermal corrections (at 298 K) obtained from HF harmonic vibrational frequencies. Free energies include entropic contributions obtained at the same level)

Reaction	E_{act}			$\Delta G^{\neq}$		
	HF	MP2	B3LYP	HF	MP2	B3LYP
TME+$^1O_2$ *Anti* Me H-abstraction	14.61	−8.53	−16.63	26.64	4.10	−3.99
TME+$^1O_2$ *Syn* Me H-abstraction	15.45	−8.35	−16.13	27.60	4.41	−3.36
TME+$^1O_2$ Mono Me H-abstraction	17.46	−10.95	−15.13	30.15	2.33	−1.85
$Li^+\cdots$TME+$^1O_2$ *Anti* Me H-abstraction	46.50	0.56	3.49	58.35	12.41	15.35
$Li^+\cdots$TME+$^1O_2$ *Syn* Me H-abstraction	47.82	−0.48	2.65	59.86	11.56	14.69
$Li^+\cdots$TME+$^1O_2$ Mono Me H-abstraction	44.57	−2.94	0.07	56.78	9.27	12.28

level calculations,[33b,c] the barrier for hydrogen abstraction is relatively low at the MP2 level. The step is indicated to be a downhill process at the B3LYP level. Evidently, the regioselectivity in the parent olefin is determined by other steps of the PE surface, e.g. formation of the biradical intermediate or more likely a pathway involving a perepoxy intermediate and/or an exciplex.

Of more interest in the present context is the effect of lithium coordination on the nature of the ene transition state. The computed geometry is markedly different in character (Table 6, Fig. 7). The ene reaction in the presence of a lithium cation is indicated to be a much more concerted process. For all three regioisomeric forms, the newly formed C–O bond is quite long (ca. 1.9 Å compared to 1.4 Å without the cation). Further, the migrating hydrogen is partially bound nearly equally to both the carbon and oxygen atoms (C1–H6 and O5–H6, Table 6). The dramatic change in the

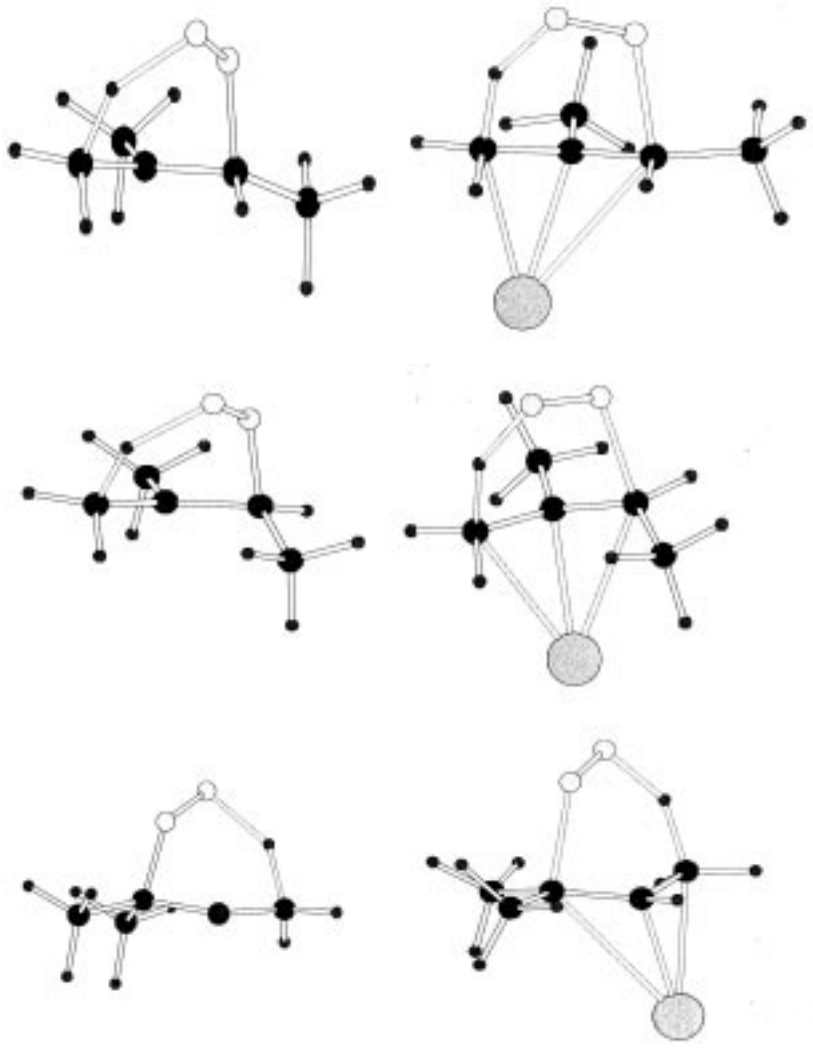

Figure 7. HF/6-31G** optimized transition state structures for hydrogen abstraction from 2-methyl-2-butene (left) and its Li^+ complex (right) by singlet oxygen. The top, middle and bottom rows correspond to *anti*, *syn* and mono methyl hydrogen abstraction, respectively. For the definition of *anti*, *syn* and mono methyl see Scheme 1.

geometric parameters is a direct consequence of lithium coordination. A more concerted process enables the metal to maintain its strong interaction with the pi unit of the alkene, which rearranges from C2–C3 to C1–C2 during the course of the reaction. This is not possible in alternative pathways involving the formation of biradical, zwitterionic or perepoxy intermediates in which no C=C bond is available for interaction with the metal.

Metal coordination has an important energetic consequence as well. The computed activation energies as well as free energies are substantially higher. Cation–pi interaction reduces the reactivity of the olefin towards electrophiles. At both the MP2 and B3LYP levels, formation of the tertiary hydroperoxide by hydrogen abstraction from the mono-methyl group of trimethylethylene is calculated to be favored by a small margin. Between the gem-dimethyl units, abstraction from the *syn* methyl group is slightly favored compared to the *anti* counterpart. These trends are not compatible with the observed regioselectivities for the ene reactions of **9** and **12**. The experimental observations and results of current theoretical calculations do not agree. We are currently looking into the discrepancies between the two results.

Summary and outlook

Thiazine dyes such as thionin, methylene blue and methylene green have been cation exchanged within monovalent cation exchanged Y zeolites. Depending on the water content the dye molecules exist as either monomers ('dry') or dimers ('wet'). The monomeric dye upon excitation with visible light generates singlet oxygen, which has been utilized to oxidize alkenes to hydroperoxides. The oxidation within zeolites is accompanied by photodecomposition of the dye and the product hydroperoxides and acid catalyzed rearrangement of alkenes. Care must therefore be taken to neutralize the acid sites with pyridine prior to including alkenes that are acid sensitive.

Our experimental results on unsymmetrical olefins clearly reveal cation-dependent regioselective hydroperoxidation. Ab initio and DFT calculations on model systems confirm fairly strong cation–alkene binding as well as additional geometric and orbital distortions. Computed activation energies for hydrogen abstraction suggest a significant rate retardation due to metal coordination. While the trend is reasonable, it is unlikely to preclude oxidation in a zeolite since the cation effect is expected to be reduced by coordination of the metal ion to the oxygen framework. Further, the singlet oxygen species may be longer lived in the confines of a zeolite cavity enabling it to overcome the necessary barrier for the ene reaction.

The steric constraints imposed by additional coordination sites around the cation may account for the difference in the computed and observed regioselectivities. However, alternative scenarios can be envisaged to resolve the discrepancy between the observed and calculated regioselectivities. Instead of the concerted pathway, which enables the cation to interact with the alkene π unit throughout the course of the ene reaction, the cation could migrate to the negatively charged oxygen of the perepoxy or zwitterionic intermediates. Such structures, in turn, may control the preferred sites of hydrogen abstraction. If the rearrangement of the cation from the olefin π face to the oxygenating species involves a barrier, the participation of a second cation interacting with the oxygen atoms and directing the course of the reaction can be postulated. In this context it is worth recalling that the Y zeolites contain four Type II cations within a supercage where the oxidation is presumed to take place. Yet another interpretation is that the oxidation process is initiated with the unbound alkene and the cation gets involved only at the stage of the perepoxy or zwitterionic intermediate. We are currently carrying out additional experimental and theoretical studies to narrow down these possibilities.

Experimental

Materials

Hexane and acetonitrile (Fischer scientific) were used without further distillation. Tetrahydrofuran and diethyl ether (Fischer scientific) were distilled to remove the peroxide impurities prior to use. All olefins used in this investigation were commercial samples (Aldrich or Chemsampco) and were distilled once prior to use. Thionin (Aldrich), methylene blue (Eastman), methylene green (Fluka), NaY (CBV-100) zeolite (Zeolyst International) were used as received.

Preparation of M^+Y zeolites from NaY

NaY zeolite (CBV-100, Zeolyst) was exchanged with other cations (Li^+, Na^+, K^+, Rb^+, Cs^+), by refluxing 25 g of the unactivated NaY zeolite in 250 mL of 10% solution of the corresponding alkali metal nitrate for 24 h. The mixture was filtered, washed with de-ionized water and dried. The above procedure was repeated three times to ensure maximum exchange of cations of interest for Na^+ ions.

Loading dye within zeolite

Dyes were loaded on to the zeolite by stirring 5 g of the zeolite with 5 mg of the dye (thionin: 17.4 μmol or methylene blue: 15.6 μmol or methylene green: 13.7 μmol) in 250 mL of de-ionized water for 24 h. The slurry was filtered and washed thoroughly with de-ionized water until the filtrate was colorless. The zeolite residue was air dried. The loading level was approximately one molecule in 150 supercages.

General procedure for oxidation of olefins in solution

Using rose bengal as sensitizer, 12 μL of alkene in acetonitrile was irradiated using a 450 W medium pressure mercury lamp with a >420 nm filter (CS# 3-73) with continuous purging of oxygen (dried using drierite) for 20–30 min. The resulting hydroperoxides were converted to the corresponding alcohols by stirring with 25 mg (95 μmol) of triphenyl phosphine. The amount of alcohols formed was estimated using GC with 2 μL (9.4 μmol) of undecane as calibration compound. The hydroperoxides

were identified based on their ^{1}H NMR and mass spectral data and comparison with literature reports.

General procedure for oxidation of olefins within zeolite

300 mg of zeolite loaded with the dye was dried in an oven at 120°C for 24 h or under vacuum (10^{-3} Torr) at 60°C for 4–5 h. The dried zeolite/dye was added to a test tube containing 12 mL of hexane and 12 μL of alkene. The hexane–zeolite/dye slurry was irradiated using a 450 W medium pressure mercury lamp with a >420 nm filter (CS# 3-73) with stirring and continuous purging of oxygen (dried using drierite) for a given time interval. The slurry was then filtered and the filtrate (hexane supernatant) was analyzed using GC with 2 μL (9.4 μmol) of undecane (calibration compound) to estimate the amount of the unreacted alkene. The zeolite residue was then extracted three times with 5 mL of acetonitrile. The extracted hydroperoxides were converted to the corresponding alcohols by stirring with 25 mg (95 μmol) of triphenylphosphine. The amount of alcohols formed was estimated using GC with 2 μL (9.4 μmol) undecane (calibration compound). The hydroperoxides were identified using both ^{1}H NMR and mass spectral data.

Testing the photostability of hydroperoxides within zeolites

Using rose bengal as the sensitizer, 12 μL of alkene in acetonitrile was irradiated using a 450 W medium pressure mercury lamp with a >420 nm filter (CS# 3-73) with continuous purging of oxygen for 1 h. Acetonitrile was evaporated and the resulting residue was stirred with hexane and passed through a cotton plug to remove rose bengal. The resulting colorless hexane solution containing the hydroperoxides was divided into two equal parts. Undecane (2μL, 9.4 μmol — calibration compound) was added to the first part to estimate the initial amount of hydroperoxides analyzed as alcohols using GC. To the second part, dried dye exchanged zeolite was added and irradiated using a 450 W medium pressure mercury lamp with a >420 nm filter (CS# 3-73) with continuous purging of oxygen (dried using drierite) for given time intervals. The slurry was then filtered and the filtrate (hexane supernatant) was analyzed using GC with 2 μL (9.4 μmol) of undecane (calibration compound) to check the presence of the hydroperoxides (hydroperoxides were not detected). The zeolite residue was then extracted three times with 5 mL of acetonitrile to obtain the hydroperoxides. The hydroperoxides were converted to the corresponding alcohols by stirring with 25 mg (95 μmol) of triphenylphosphine. The amount of alcohols formed was estimated using GC with 2 μL (9.4 μmol) of undecane as the calibration compound. The decomposition of hydroperoxides was estimated by comparing the amount of hydroperoxides (as alcohols), before (first part) and after (second part) the reaction.

Testing the photostability of dyes included in zeolites

Photostability was monitored by recording the diffuse reflectance spectrum of the sample irradiated for different time intervals. Diffuse reflectance spectra were recorded by packing the samples in a 1 mm quartz cell. The background correction was carried out using barium sulfate in the same cell. The recorded spectrum for the sample was converted into Kubelka–Munk units by the program supplied with the instrument (Shidmadzu UV–Vis scanning spectrophotometer UV-2101PC). The dried zeolite/dye samples were packed in the quartz cell and sealed with the stopper inside the dry box. The decomposition of the dye (thionin, methylene blue, methylene green) inside various MY zeolites (M=Li^+, Na^+, K^+, Rb^+, Cs^+) with irradiation at different time intervals was followed by diffuse reflectance spectra using the same baseline correction.

Irradiation of zeolite/dye samples with oxygen purging

300 mg of zeolite/dye was dried under vacuum (10^{-3} Torr) at 60°C for 4–5 h and transferred into test tubes containing 12 mL of hexane and sealed with rubber septa. The hexane–zeolite/dye slurries were irradiated using a 450 W medium pressure mercury lamp with a >420 nm filter (CS# 3-73) with continuous purging of oxygen (dried using drierite) for various time intervals. The hexane–zeolite/dye slurries were filtered, air dried and transferred immediately into 1 mm quartz cells and stoppered. Diffuse reflectance spectra of zeolite/dye samples packed inside the quartz cell were recorded (Kubelka–Munk units) using the same baseline correction (carried out using barium sulfate in the same cell). The absorbance of the sample which was not irradiated was taken as 100% and the relative absorbances of the irradiated samples were calculated.

Irradiation of zeolite/dye samples with nitrogen purging

300 mg of zeolite/dye was dried under vacuum (10^{-3} Torr) at 60°C for 4–5 h and transferred into test tubes containing 12 mL of hexane and sealed with rubber septa. The hexane–zeolite/dye slurries were irradiated using a 450W medium pressure mercury lamp with a >420 nm filter (CS# 3-73) with continuous purging of nitrogen (dried using drierite) for various time intervals. The hexane–zeolite/dye slurries were filtered, air dried and transferred immediately into 1 mm quartz cells and stoppered. Diffuse reflectance spectra of zeolite/dye samples packed inside the quartz cell were recorded (Kubelka–Munk units) using the same baseline correction (carried out using barium sulfate in the same cell). The absorbance of the sample which was not irradiated was taken as 100% and the relative absorbances of the irradiated samples were calculated.

Acknowledgements

The authors at Tulane University thank the Division of Chemical Sciences, Office of Basic Sciences, US Department of Energy (DE-FGOR-96ER14635) for support of this program, W. Adam and E. Clennan for critical comments on our results, for useful discussions and for sharing unpublished data. R. B. S. thanks CSIR (New Delhi) for a research fellowship.

References

1. (a) Griesbeck, A. G. *CRC Handbook of Organic Photochemistry*

and Photobiology; 1995; pp 301–310. (b) Wasserman, H. H., Murray, R. W., Eds.; *Singlet Oxygen*; Academic: New York, 1979. (c) Frimer, A. A. Ed. *Singlet Oxygen*; CRC: Boca Raton, 1985; Vols. 1–4.
2. (a) Frimer, A. A.; Stephenson, L. M. *Singlet Oxygen*; Frimer, A. A., Ed.; CRC: Boca Raton, 1985; pp 67–92. (b) Gollnick, K.; Kuhn, H. J. *Singlet Oxygen* Wasserman, H. H., Murray, R. W., Eds.; Academic: New York, 1979; pp 287–429.
3. Prein, M.; Adam, W. *Angew. Chem., Int. Ed. Engl.* **1996**, *35*, 477.
4. (a) Frimer, A. A. *Chem. Rev.* **1979**, *79*, 359. (b) Stephenson, L. M.; Grdina, M. J.; Orfanopoulous, M. *Acc. Chem. Res.* **1980**, *13*, 419. (c) Stephenson, L. M. *Tetrahedron Lett.* **1980**, *21*, 1005. (d) Houk, K. N.; Williams, J. C., Jr.; Mitchell, P. A.; Yamaguchi, K. *J. Am. Chem. Soc.* **1981**, *103*, 949. (e) Jefford, C. W. *Chem. Soc. Rev.* **1993**, 59. (f) Hurst, J. R.; Schuster, G. B. *J. Am. Chem. Soc.* **1982**, *104*, 6854. (g) Stratakis, M.; Orfanopoulous, M.; Chen, J. S.; Foote, C. S. *Tetrahedron Lett.* **1996**, *37*, 4105.
5. (a) Ramamurthy, V.; Corbin, D. R.; Johnston, L. J. *J. Am. Chem. Soc.* **1992**, *114*, 3870. (b) Ramamurthy, V.; Caspar, J. V.; Kuo, E. W.; Corbin, D. R.; Eaton, D. F. *J. Am. Chem. Soc.* **1992**, *114*, 3882.
6. (a) Frei, H.; Blatter, F.; Sun, H. *Chemtech* **1996**, *26*, 24. (b) Xiang, Y.; Larsen, S. C.; Grassian, V. H. *J. Am. Chem. Soc.* **1999**, *121*, 5063.
7. (a) Breck, D. W. *Zeolite Molecular Sieves: Structure, Chemistry, and Use*; Wiley: New York, 1974. (b) Ramamurthy, V.; Robbins, R. J.; Thomas, K. J.; Lakshminarasimhan, P. H. *Organised Molecular Assemblies in the Solid State*; Whitsell, J. K., Ed.; Wiley: Chichester, 1999; pp 63–140.
8. Pettit, T. L.; Fox, M. A. *J. Phys. Chem.* **1990**, *56*, 1353.
9. (a) Li, X.; Ramamurthy, V. *Tetrahedron Lett.* **1996**, *37*, 5235. (b) Li, X.; Ramamurthy, V. *J. Am. Chem. Soc.* **1996**, *118*, 10666. (c) Robbins, R. J.; Ramamurthy, V. *Chem. Commun.* **1997**, 1071. (d) Joy. A.; Robbins, R. J.; Pitchumani, K.; Ramamurthy, V. *Tetrahedron Lett.* **1997**, 8825.
10. (a) Zhou, W.; Clennan, L. E. *J. Am. Chem. Soc.* **1999**, *121*, 2915. (b) Clennan, E. L.; Sram, J. P. *Tetrahedron Lett.* **2000**, *40*, 5275. (c) Zhou, W.; Clennan, E. L. *Org. Lett.* **1999**, *2*, 437. (d) Tung, Chen-Ho., Wang, H.; Ying, Y. M. *J. Am. Chem. Soc.* **1998**, *120*, 5179. (e) Stratakis, M. Private communication of unpublished results.
11. Ramamurthy, V.; Sanderson, D. R.; Eaton, D. F. *J. Am. Chem. Soc.* **1993**, *115*, 10438.
12. (a) Lewis, G. N.; Goldschmid, O.; Magel, T. T.; Bigeleisen, J. *J. Am. Chem. Soc.* **1943**, *65*, 1150. (b) Braswell, E. *J. Phys. Chem.* **1968**, *72*, 2477. (c) Bergmann, K.; O'Konski, C. T. *J. Phys. Chem.* **1963**, *67*, 2169. (d) Dewey, T. G.; Wilson, S. P.; Turner, H. D. *J. Am. Chem. Soc.* **1978**, *100*, 4550.
13. Calzaferri, C.; Gfeller, N. *J. Phys. Chem.* **1992**, *96*, 3428.
14. (a) Epstein, L. F.; Karush, H.; Rabinowitch, E. *J. Opt. Soc. Am.* **1941**, *31*, 77. (b) Sommer, U.; Kramer, H. E. A. *Photochem. Photobiol.* **1971**, *13*, 387.
15. Kao, H.-M.; Grey, C. P.; Pitchumani, K.; Lakshminarasimhan, P. H.; Ramamurthy, V. *J. Phys. Chem.* **1998**, *102*, 5627.
16. (a) Deeg, F. W.; Ehrl, M.; Brauchle, C.; Hoppe, R.; Schulz-Ekloff, G.; Wohrle, D. *J. Lumin.* **1992**, *53*, 219. (b) Hoppe, R.; Schulz-Ekloff, G.; Wohrle, D.; Ehrl, M.; Brauchle, C. *Zeolite Chemistry and Catalysis*; Jacobs, P. A., Ed.; Elsevier: Amsterdam, 1991; pp 199. (c) Wohrle, D.; Schulz-Ekloff, G. *Adv. Mater.* **1994**, *6*, 875. (d) Hoppe, R.; Schulz-Ekloff, G.; Wohrle, D.; Shpiro, E. S.; Tkachenko, O. P. *Zeolites* **1993**, *13*, 222.
17. Hoppe, R.; Schulz-Ekloff, G.; Wohrle, D.; Kirschhock, C.; Fuess, H.; Uytterhoeven, L.; Schoonhetdt, R. *Adv. Mater.* **1995**, *7*, 61.
18. H-aggregated dimers are known to be non-fluorescent due to the forbidden nature of transitions between the lowest excited singlet and ground states. (a) Lewis, G. N.; Goldschmid, O.; Magel, T. T.; Bigeleisen, J. *J. Am. Chem. Soc.* **1943**, *65*, 150. (b) Rabinowitch, E.; Epstein, L. F. *J. Am. Chem. Soc.* **1941**, *63*, 69. (c) Herkstroeter, W. G.; Martic, P. A.; Farid, S. *J. Am. Chem. Soc.* **1990**, *112*, 3583. (d) Sens, R.; Drexhage, K. H. *J. Lumin.* **1981**, *24*, 709. (e) Isak, S. J.; Eyring, E. M. *J. Phys. Chem.* **1992**, *96*, 1738.
19. (a) Arnold, S. J.; Ogryzlo, E. A.; Witzke, A. *J. Chem. Phys.* **1964**, *40*, 1769. (b) Kasha, M.; Brabham, D. E. *Singlet Oxygen*; Wasserman, H. H., Murray, R. W., Eds.; Academic: New York, 1979; p 1.
20. (a) Foote, C. S. *Acc. Chem. Res.* **1968**, *1*, 104. (b) Gollnik, K. *Adv. Chem.* **1968**, *77*, 78. (c) Foote, C. S.; Wexler, S.; Ando, W.; Higgins, R. *J. Am. Chem. Soc.* **1968**, *90*, 975.
21. (a) Orfanopoulos, M. PhD Thesis, Case Western Reserve University, Cleveland, OH, 1979. (b) Foote, C. S.; Denny, R. W. *J. Am. Chem. Soc.* **1971**, *92*, 5168. (c) Foote, C. S. *Pure Appl. Chem.* **1971**, *27*, 635. (d) Schulte-Elte, K. H.; Rautenstrauch, V. *J. Am. Chem. Soc.* **1980**, *102*, 1738. (e) Schulte-Elte, K. H.; Mullar, B. L.; Rautenstrauch, V. *Helv. Chim. Acta* **1978**, *61*, 2777. (f) Higgins, R.; Foote, C. S.; Cheng, H. *Adv. Chem.* **1968**, *77*, 102. (g) Orfanopoulos, M.; Grdina, Sr. B.; Stephenson, L. M. *J. Am. Chem. Soc.* **1979**, *101*, 275.
22. (a) Ohno, T.; Lichtin, N. N. *J. Phys. Chem.* **1982**, *86*, 354–360. (b) Kikuchi, K.; Kokubun, H.; Kikuchi, M. *Bull. Chem. Soc. Jpn* **1975**, *48* (5), 1378–1381. (c) Kikuchi, K.; Tamura, S.-I.; Iwanaga, C.; Kokubun, H. *Z. Physik. Chem. Neue. Folge* **1977**, *106*, 17–24. (d) Kato, S.; Morita, M.; Koizumi, M. *Bull. Chem. Soc. Jpn* **1964**, *37*, 117–124. (e) Nogueira, F. P.; Raquel, Jardim, F. W. *J. Chem. Ed.* **1993**, *70*, 861–862. (f) Kamat, P. V. *J. Photochem.* **1985**, *28*, 513–524. (g) Patrick, B.; Kamat, P. V. *J. Phys. Chem.* **1992**, *96*, 1423–1428. (h) Liu, D.; Kamat, P. V. *Langmuir* **1996**, *12*, 2190–2195. (i) Gopidas, K. R.; Kamat, P. V.; George, M. V. *Mol. Cryst. Liq. Cryst.* **1990**, *183*, 403–409. (j) Krishna, R. M.; Prakash, A. M.; Kevan, L. *J. Phys. Chem. B* **2000**, *104*, 1796–1801.
23. (a) Hashimoto, S. *J. Chem. Soc. Trans. Faraday Soc.* **1997**, *93*, 4401. (b) Liu, X.; Iu, K.-K.; Thomas, J. K. *J. Phys. Chem.* **1994**, *98*, 7877. (c) Liu, X.; Iu, K.-K.; Thomas, J. K. *Chem. Phys. Lett.* **1993**, *204*, 163. (d) Alvaro, M.; Garcia, H.; Garcia. S.; Márquez. F.; Scaiano, J. C. *J. Phys. Chem. B* **1997**, *101*, 3043. (e) McManus, H. J. D.; Finel, C.; Kevan, L. *Radiat. Phys. Chem.* **1995**, *45*, 761.
24. Thomas, K. J.; Ramamurthy, V. *Langmuir* **1998**, *14*, 6687.
25. The GAUSSIAN 94 suite of programs were used for all the calculations: Frisch, M. J.; Trucks, G. W.; Schlegel, H. B.; Gill, P. M. W.; Johnson, B. G.; Robb, M. A.; Cheeseman, J. R.; Keith, T.; Petersson, G. A.; Montgomery, J. A.; Raghavachari, K.; Al-Laham, M. A.; Zakrzewski, V. G.; Ortiz, J. V.; Foresman, J. B.; Cioslowski, J.; Stefanov, B. B.; Nanayakkara, A.; Challacombe, M.; Peng, C. Y.; Ayala, P. Y.; Chen, W.; Wong, M. W.; Andres, J. L.; Replogle, E. S.; Gomperts, R.; Martin, R. L.; Fox, D. J.; Binkley, J. S.; Defrees, D. J.; Baker, J.; Stewart, J. P.; Head-Gordon, M.; Gonzalez, C.; Pople, J. A. GAUSSIAN 94, Revision C.2; Gaussian: Pittsburgh, PA, 1995.
26. Hehre, W. J.; Radom, L.; Schleyer, P. V. R.; Pople, J. A. *Ab-Initio Molecular Orbital Theory*, Wiley: New York, 1986.
27. Hay, J. P.; Wadt, W. R. *J. Chem. Phys.* **1985**, *82*, 299.
28. (a) Ma, J. C.; Dougherty, D. A. *Chem. Rev.* **1997**, *97*, 1303. (b) Dougherty, D. A. *Science* **1996**, *271*, 163.

29. Nicholas, J. B.; Hay, B. P.; Dixon, D. A. *J. Phys. Chem. A* **1999**, *103*, 1394.
30. Setzer, W.; Schleyer, P. V. R. *Adv. Organomet. Chem.* **1985**, *24*, 353.
31. Imagaki, S.; Fukui, K. *J. Am. Chem. Soc.* **1975**, *97*, 7480.
32. (a) Maranzana, A.; Ghigo, G.; Tonachini, G. *J. Am. Chem. Soc.*, **2000**, *122*, 1414. (b) Liwo, A.; Dyl, D.; Jeziorek, D.; Nowacka, M.; Ossowski, T.; Woznicki, W. *J. Comput. Chem.* **1997**, *18*, 1668. (c) Harding, L. B.; Goddard, W. A., III. *Tetrahedron Lett.* **1978**, *8*, 747. (d) Tonachini, G.; Schlegel, H. B.; Bernardi, F.; Robb, M. A. *J. Am. Chem. Soc.* **1990**, *112*, 483. (e) Hotokka, M.; Roos, B.; Siegbahn, P. *J. Am. Chem. Soc.* **1983**, *105*, 5263. (f) Yamaguchi, K.; Yabushita, S.; Fueno, T.; Houk, K. N. *J. Am. Chem. Soc.* **1981**, *103*, 5043. (g) Harding, L. B.; Goddard, W. A., III, *J. Am. Chem. Soc.* **1977**, *99*, 4520. (h) Dewar, M. J. S.; Griffin, A. C.; Thiel, W.; Turchi, I. J. *J. Am. Chem. Soc.* **1975**, *97*, 4430.
33. (a) Dewar, M. J. S.; Thiel, W. *J. Am. Chem. Soc.* **1975**, *97*, 3978. (b) Harding, L. B.; Goddard, W. A., III. *J. Am. Chem. Soc.* **1980**, *102*, 439. (c) Yoshioka, Y.; Yamada, S.; Kawakami, T.; Nishino, M.; Yamaguchi, K.; Saito, I. *Bull. Chem. Soc. Jpn* **1996**, *69*, 2683.